Research Square

Preprints are preliminary reports that have not undergone peer review.
They should not be considered conclusive, used to inform clinical practice,
or referenced by the media as validated information.

Synthesis, In Vitro Antimicrobial and In Silico Studies of Aminoalkyl Derivatives of Carvacrol

Asaminew Goa

asaminew.goa@wsu.edu.et

Addis Ababa University

Avijit Mazumder

Noida Institute of Engineering and Technology

Kaleab Asres

Addis Ababa University

Daniel Bisrat

Addis Ababa University

Article

Keywords: Carvacrol, Aminoalkyl, Antimicrobial, Antimicrobial Resistance, In Silico study

Posted Date: May 5th, 2026

DOI: https://doi.org/10.21203/rs.3.rs-9414478/v1

License: This work is licensed under a Creative Commons Attribution 4.0 International License.
Read Full License

Additional Declarations: No competing interests reported.

Abstract

The global rise of antimicrobial resistance has created an urgent need for the development of new antimicrobial agents. Carvacrol, a natural phenolic compound, has drawn significant attention in medicinal chemistry due to its broad-spectrum biological activities. In the present study, two novel aminoalkyl derivatives of carvacrol were successfully synthesized through a Mannich-type reaction, which involves the condensation of carvacrol with formaldehyde and a secondary amine (dimethylamine or piperdine). Structural confirmation of the synthesized derivatives was carried out using spectroscopic techniques (1H-NMR and 13C-NMR). Based on the spectral data, the compounds were identified as 4-((dimethylamino)methyl)-5-isopropyl-2- methylphenol (2) and 5-isopropyl-2-methyl-4-(piperidin-1-ylmethyl)phenol (3). These compounds were evaluated for their in vitro antimicrobial activity against twenty-six bacterial strains and four fungal strains by using disc diffusion and broth dilution methods. Both compound 2 and 3 demonstrated a broad antimicrobial activity. Specifically, Compound 3 exhibited the highest antibacterial activity against Escherichia coli and Vibrio cholerae strains with a lower MIC value (25 µg/mL) and also showed superior antifungal activity against Candida albicans and Penicillium funiculosum NCTC 287 (MIC: 200 µg/mL). Furthermore, both compounds were evaluated through in silico studies to predict their potential mechanisms of action and assess their drug-likeness properties. Among the two, compound 2 exhibited the strongest binding affinity, with a docking score of -5.677kJ/mol against the target protein enoyl- acyl carrier protein reductase (FabI), a crucial enzyme in bacterial fatty acid biosynthesis. This work suggests that the aminoalkyl derivatives of carvacrol could be promising candidates for the development of new antimicrobial drugs that combat infections and help combat antimicrobial resistance.

Introductions

Infectious diseases, caused by harmful microorganisms such as bacteria, viruses, fungi, and parasites, have been a significant cause of morbidity and mortality throughout human history. These diseases occur when pathogens invade the body, multiply, and disrupt normal biological functions, often resulting in a variety of symptoms ranging from mild to severe [1,2]. Despite advancements in medicine, infectious diseases remain a significant global health concern, particularly in low-income countries and among vulnerable populations such as young children. According to a 2007 WHO report, infectious diseases are spreading rapidly than ever before and new infectious diseases are being found more frequently than ever before [3]. In 2019, the Global Comprehensive Estimates of the Burden of Bacterial Infections reported that bacterial infections caused about 7.7 million deaths worldwide, making them the second leading cause of death after ischemic heart disease [4]. Fungal diseases also represent a significant global health burden, affecting over one billion people and causing more than 1.5 million deaths annually, particularly among immunocompromised patients such as those with cancer, AIDS, or organ transplants [5,6].

Natural products remain valuable sources of new therapeutic agents with diverse mechanisms of action against resistant pathogens. Among them, carvacrol, a monoterpenoid phenol abundant in the essential

oils of oregano and other aromatic plants, exhibits notable antimicrobial activity [7]. However, its clinical application is limited by volatility, low aqueous solubility, and poor bioavailability [8]. To overcome these limitations and enhance biological activity, chemical modification through the Mannich-type reaction, which introduces aminoalkyl groups via condensation with formaldehyde and amines, has been explored [9].

Materials and Methods

Chemicals and Instruments

Carvacrol, methanol (99.9%), ethanol (99.9%), formaldehyde (37%), chloroform (99.8%), anhydrous sodium sulfate, dimethyl amine, piperidine, and glacial acetic acid (all from Sigma-Aldrich Co., MO, USA). All the solvents and reagents are of analytical grade.

Thin-layer chromatography (TLC) was carried out using silica gel plates (60 F254, 0.2 mm, Merck KGaA, Darmstadt, Germany) and visualized under UV light using an Evolution 60S UV–Visible Spectrophotometer. NMR spectra were recorded on a Bruker Avance DMX400 FT NMR Spectrometer (400 MHz for ^{1}H and 100 MHz for ^{13}C) using $CDCl_3$ as solvent and tetramethylsilane (TMS) as internal standard.

Synthesis of aminoalkyl derivatives of carvacrol (2 and 3)

4-((Dimethylamino) methyl)-5-isopropyl-2-methylphenol (2)

The general procedure for the synthesis of compound **2** was as follows: a solution of 0.75 ml (0.01 mol) of 37% aqueous formaldehyde in 10 ml of methanol was prepared in a 50 ml beaker, with five drops of acetic acid as a catalyst. Dimethylamine (0.66 ml, 0.01 mol) was added dropwise to a solution of formaldehyde and acetic acid to form an iminium intermediate, which was then added dropwise to a solution of carvacrol (1.5g, 0.01 mol) in methanol. The resulting mixture was thoroughly stirred and refluxed in a 250 ml Erlenmeyer flask for 28 hours at 100°C. The reaction progress was monitored using TLC with a chloroform/ methanol (4:1) solvent system. After refluxing, the mixture was cooled to room temperature and poured into ice-cold water to precipitate the product, followed by overnight storage in a refrigerator to enhance precipitation. The resulting precipitate was filtered, washed with ethanol, and dried over anhydrous sodium sulfate ($Na_2SO_{4)}$. Finally, the product is purified through recrystallization in ethanol to obtain the pure compound **2**.

4-((Dimethylamino)methyl)-5-isopropyl-2-methylphenol (**2**): colorless crystals; 85%, w/w; Rf = 0.45 ($CHCl_3$/MeOH). ^{1}H NMR (400 MHz, $CDCl_3$): H-3 (δ 6.99, 1H, s), H-6 (δ 6.56, 1H, s), H-7 (δ 2.13, 3H, s), H-8 (δ 3.21, 1H, m), H-9 and H-9' (δ 1.10, 6H, d, J = 8 Hz), H-10 (δ 3.38, 2H, s), H-12 and H-12' (δ 2.25, 6H, s); ^{13}C NMR (100 MHz, $CDCl_3$): C-1 (153.93), C-2 (121.09), C-3 (133.44), C-4 (126.42), C-5 (147.01), C-6 (111.89), C-7 (15.48), C-8 (28.26), C-9 and C-9' (23.99), C-10 (60.25), C-12 and C-12' (45.30).

5-Isopropyl-2-methyl-4-(piperidin-1-ylmethyl) phenol (3)

Compound **3** was synthesized following a procedure similar to that used for compound **2**. A solution of 37% aqueous formaldehyde (0.75 mL, 0.01 mol) in 10 mL of methanol was prepared with five drops of acetic acid as a catalyst. Piperidine (1 mL, 0.01 mol) was added dropwise to form the iminium intermediate, which was then added dropwise to a methanolic solution of carvacrol (1.5 g, 0.01 mol). The reaction mixture was stirred and refluxed at 100°C for 20 hours, with reaction progress monitored by TLC. After refluxing, the mixture was cooled and poured into ice-cold water, then stored overnight in the refrigerator. The resulting precipitate was filtered, washed with ethanol, dried over anhydrous Na_2SO_4, and recrystallized from ethanol to obtain pure compound **3**.

5-Isopropyl-2-methyl-4-(piperidin-1-ylmethyl)phenol (**3**): colorless crystals; 66%, w/w; Rf = 0.55 ($CHCl_3$/MeOH). ^{1}H NMR (400 MHz, $CDCl_3$): H-3 (δ 7.15, 1H, s), H-6 (δ 6.72, 1H, s), H-7 (δ 2.25, 3H, s), H-8 (δ 3.17, 1H, m), H-9 and H-9' (δ 1.26, 6H, d, J = 8 Hz), H-10 (δ 3.75, 2H, s), H-2' and H-6' (δ 2.62, 4H, t), H-3' and H-5' (δ 1.66, 4H, m), H-4' (δ 1.47, 2H, m).; ^{13}C NMR (100 MHz, $CDCl_3$): C-1 (153.30), C-2 (128.51), C-3 (133.86), C-4 (129.53), C-5 (138.08), C-6 (120.43), C-7 (20.34), C-8 (28.25), C-9 and C-9' (23.76), C-10 (58.66), C-2' and C-6' (55.53), C-3' and C-5' (26.73), C-4' (25.10).

Spectroscopic analysis of the synthesized compounds

The structures of compounds **2** and **3** were identified by analyzing their ^{1}H and ^{13}C-NMR

spectra data. Chemical shifts are denoted in parts per million (*ppm)* and coupling constants (*J*) are expressed in *Hz*. Signal multiplicities are indicated as follows: *s* = singlet; *d* = doublet; *t* = triplet; and *m* = multiplet.

In vitro antibacterial and antifungal activity assay

Disc Diffusion Method

The disc diffusion method was used to screen the *in vitro* antibacterial assay by comparing the zones of inhibition generated by the test samples with those of ciprofloxacin [10]. To investigate the synthesized compounds, 200 µg/mL of each of the test samples dissolved in 1% DMSO and ciprofloxacin dissolved in sterile distilled water were prepared. After that, sterile Petri dishes were filled with molten nutrient agar to create agar plates, which were then incubated at 37°C for 24 hours to check for contamination. Once sterility was confirmed, the surface of each agar plate was uniformly inoculated with standardized bacterial suspensions adjusted to 0.5 McFarland standards using a sterile cotton swab. Sterile filter paper discs (Whatman No. 1) with diameter 6 mm were then immersed in the test sample stock solution (200 µg/mL) and carefully placed on the surface of an agar plate. After being incubated for 24 hours at 37°C, the diameter of the zones of inhibition (ZOI) in the petri dishes was measured in millimeters. A similar procedure was applied to pure ciprofloxacin, and the corresponding zone of inhibition was

appropriately compared. 1% DMSO was used as a negative control [11]. For antifungal activity, a similar protocol was followed using Sabouraud Dextrose Agar (SDA) as the growth medium. The fungal pathogens were inoculated, and the plates were incubated for three days at room temperature. After incubation, the ZOI diameters were measured in millimeters. In this assay, Griseofulvin was used as the standard for comparison.

Broth Dilution Method

The minimum inhibitory concentrations (MICs) of the synthesized compounds were investigated by using broth dilution methods described by Jean B.etal (2015). Mueller–Hinton broth and Saborauds dextrose broth were used for bacterial and fungal growth, respectively. A broth with varying concentrations of the test sample ranging from 5 to 800 µg/mL for antibacterial activity testing and 50 to 2000 µg/mL for antifungal activity testing was made. 1% DMSO was used to dissolve the synthesized compounds. Furthermore, a growth control (nutrient broth with DMSO and inoculum, without antimicrobial agents) was included to confirm microbial viability, while a sterility control (nutrient broth with DMSO, without inoculum or antimicrobials) was included to ensure the absence of contamination. Each test and control well was incubated at 37°C for 24 hours for bacteria and at 25°C for three days for fungi. The MIC was identified as the lowest concentration that inhibited visible growth, indicated by the absence of turbidity in the wells [13].

In silico studies

Molecular docking study

Molecular docking studies were performed with Maestro v13.5 of the Schrödinger 2023-1 Suite to determine the possible interaction of the synthesized compounds with the enoyl-acyl carrier protein reductase enzyme FabI, a key target in the fatty acid biosynthesis pathway in bacteria. The crystal structure of FabI of *E. coli* (PDB ID: 1C14), with a resolution of 2.00 Å, was obtained from the Protein Data Bank (PDB) and used for docking studies to assess the potential of the synthesized compounds as FabI inhibitors.

Protein preparation

The molecular docking procedure first involved preparing the FabI (PDB ID: 1C14) 3D structure using the Protein Preparation Wizard in Maestro. As part of the preparation, unnecessary components such as water molecules were removed so they would not affect ligand binding. Next, hydrogen atoms were added to the structure, correcting errors such as absent side chains, allocating appropriate bond ordering, correcting charges and atom types, and filling in missing side chains and loops. The Optimized Potentials for Liquid Simulations 4 (OPLS4) force field was applied for energy minimization to optimize molecular geometry and reduce steric clashes [14].

Ligand preparation

Ligand preparation was performed using Schrödinger's LigPrep module. Structures were drawn in ChemDraw ultar12.0 and imported into LigPrep for conversion from 2D to 3D, with hydrogen addition, computing correct partial charges, optimizing the structures, and achieving the appropriate protonation states at physiological pH 7.0 ± 2.0 by using Epik [15]. LigPrep also generated relevant ionization states, tautomers, and ring conformations for docking studies.

Receptor Grid Generation

Maestro v13.5's Grid Generation module was used to create the receptor. The grid was a cubic box, centered on the active site originally occupied by the co-crystallized ligand, which was excluded during the process. This approach ensured that new compounds could be docked precisely at the same binding site. The setup was specifically designed to facilitate the docking studies of amino alkyl carvacrol derivatives, allowing evaluation of their potential interactions within the defined binding pocket.

Ligand docking

Using the Glide tool in Maestro, molecular docking simulations were performed under extra precision (XP) modes. Ligands were docked into the FabI active site. The XP mode applied tighter scoring functions and constraints for improved accuracy. The Van der Waals scaling factor and partial charge cut-off for ligand atoms were adjusted to 0.80 and 0.15, respectively. Docking scores were used to estimate binding affinities by evaluating key interactions, such as hydrogen bonds, electrostatic, and hydrophobic interactions. To ensure reliability, redocking was performed by reintroducing the co-crystallized ligand into the active site of FabI and evaluating its binding affinity.

Drug-likeness, Pharmacokinetics, and Toxicity Studies

The drug-likeness, pharmacokinetic, and toxicity profiles of the synthesized compounds were predicted using online ADMETlab 3.0. The 2D structures were drawn in ChemDraw Ultra 12.0, and their SMILES strings were generated and submitted to the ADMETlab 3.0 web server to evaluate absorption, distribution, metabolism, excretion, toxicity (ADMET), and drug-likeness.

Results and discussion

Synthesis of aminoalkyl derivatives of carvacrol (2 and 3)

In this study, two aminoalkyl derivatives of carvacrol were successfully synthesized through a Mannich-type reaction in which carvacrol reacted with formaldehyde and two secondary amines, dimethylamine and piperidine, resulting in the formation of aminoalkylated products. The overall synthetic route is shown in Scheme 1.

Compound **2**, 4-((dimethylamino)methyl)-5-isopropyl-2-methylphenol, was synthesized via a one-pot Mannich reaction involving the condensation of carvacrol, formaldehyde, and dimethylamine in the presence of acetic acid as an acid catalyst. The reaction mechanism involved the protonation of formaldehyde followed by nucleophilic attack of dimethylamine to generate an iminium ion intermediate. This intermediate subsequently reacted with the electron-rich aromatic ring of carvacrol through electrophilic aromatic substitution at the para position relative to the hydroxyl group, producing compound **2**. The proposed reaction mechanism is presented in Scheme 2. Compound **3**, 5-isopropyl-2-methyl-4-(piperidin-1-ylmethyl) phenol, was synthesized using the same Mannich reaction procedure by replacing dimethylamine with piperidine. The reaction followed a similar pathway involving the formation of an iminium ion intermediate and electrophilic substitution on the aromatic ring of carvacrol.

Scheme 2: A Proposed reaction mechanism for the formation of aminoalkyl derivatives of carvacrol.

Structural elucidation of compounds 2 and 3

Compounds **2** and **3** were identified as 4-((dimethylamino)methyl)-5-isopropyl-2-methylphenol and 5-isopropyl-2-methyl-4-(piperidin-1-ylmethyl) phenol, respectively, based on the analysis of their ^{1}H and ^{13}C-NMR spectral data. Detailed spectral data are provided in the Material and Methods section. The ^{1}H-NMR spectrum data (Supplementary Fig.S1) of compound **2** showed two aromatic proton signals corresponding to H-6 (δ 6.56, ArH, s) and H-3 (δ 6.99, ArH, s), indicating that one aromatic proton of carvacrol was replaced by an aminoalkyl group. A singlet at δ 3.38 (2H, s) indicated the presence of a methylene group attached to a nitrogen atom, confirming the formation of the aminoalkyl group. The ^{13}C-NMR spectrum (Supplementary Fig.S2) revealed a total of thirteen carbon atoms consisting of four quaternary carbons, five methyl carbons, three methine carbons, and one methylene carbon. The methylene carbon linking the aromatic ring to the dimethylamino group appeared at δC 60.26 ppm.

Similarly, the ^{1}H-NMR spectrum (Supplementary Fig.S3) of compound **3** displayed two aromatic proton signals at H-6 (δ 6.72, 1H, s) and H-3 (δ 7.15, 1H, s), confirming substitution on the aromatic ring. A singlet at δ 3.75 ppm corresponded to the methylene group linking the aromatic ring to the piperidine moiety, while signals at δ 2.62, 1.47, and 1.66 ppm were assigned to protons within the piperidine ring. The ^{13}C-NMR spectrum (Supplementary Fig.S4) confirmed the presence of 16 carbon atoms, including four quaternary carbons, three methyl carbons, three methine carbons, and six methylene carbons. The methylene carbon linking the aromatic ring to the piperidine moiety appeared at δC 58.66 ppm, while the piperidine carbons appeared at δC 25.1–55.53 ppm.

Antimicrobial activity of compound 2 and 3

Antibacterial activity

The antibacterial activity of compounds **2** and **3** was evaluated against 26 bacterial strains, including Gram-negative and Gram-positive bacteria, using the disc diffusion assay and broth dilution method. Ciprofloxacin, a well-established broad-spectrum antibiotic, was included in the study as a positive control. Both compounds demonstrated comparable antibacterial activity against a broad range of

bacterial strains, with ZOIs ranging from 6 to 16 mm and MICs ranging from 25µg/mL to 400µg/mL (Table 1). Overall, compound **3** demonstrated greater antibacterial potency than compound **2**, showing larger inhibition zones and lower MIC values against several bacterial strains. Among the tested strains, the strongest activity was observed against multiple *E. coli* isolates, with ZOI reaching up to 16.0 mm in diameter and exhibited MIC values as low as 25µg/mL against these strains, indicating strong antibacterial efficacy. This finding is notable because *E. coli* is a major causative agent of urinary tract infections, gastroenteritis, renal failure, and sepsis [16], and many strains have developed multidrug resistance to currently available antibiotics [17]. Moderate antibacterial activity was observed against *Salmonella enterica* and *Shigella* species, with inhibition zones of 11.5–13.5 mm and MIC values of 100–200 µg/mL. Both compounds also demonstrated strong activity against *Vibrio cholerae*, one of the most dangerous bacterial pathogens, commonly associated with severe diarrheal diseases in both humans and animals. In its acute form, cholera can lead to hypovolemia, potentially resulting in shock and death if left untreated [18].The compounds produced inhibition zones of 14–16 mm and MIC values between 25–50 µg/mL, indicating high susceptibility of this species. In contrast, neither compound showed activity against *Bacillus pumilus* 82 or *Bacillus subtilis* ATCC 6633. Against multidrug-resistant strains of *Staphylococcus aureus*, compound **3** showed weak activity toward MDR1 and MDR2 (MIC = 400 µg/mL), whereas both compounds exhibited stronger activity against the MDR10 strain (MIC = 50 µg/mL). These findings suggest limited potency against certain Gram-positive resistant strains. In general, Gram-positive bacteria showed greater resistance to the compounds **2** and **3** compared to Gram-negative strains. Particularly, compound **3** demonstrated high activities against Gram-negative bacteria such as *E. coli* and *V. cholera*.

Antifungal activity

Both synthesized compounds demonstrated antifungal activity against four fungal strains, with zones of inhibition ranging from 10.5 to 14.5 mm and MIC values between 200 and 800 µg/mL as summarized in Table 2. Overall, compound **3** exhibited stronger antifungal activity than compound **2** across all tested strains. Among the fungi evaluated, *Candida albicans* ATCC 10231 (ZOI = 14.5mm and MIC = 200 µg/mL) and *Penicillium funiculosum* NCTC 287 (ZOI = 13.5mm and MIC = 200) were the most susceptible to compound **3**, showing the largest zone of inhibition (14.5 mm) and the lowest MIC (200 µg/mL), indicating notable antifungal potency. A comparative assessment of both compounds revealed differences in activity levels against the tested fungal strains (Table 2).

Table 1
Zone of inhibition and minimum inhibitory concentration of the compound **2** and **3** against the tested bacterial strains

Name of Bacteria	**Zone of inhibition in mm (200 µg/ml)**			**MIC (µg/ml)**	
	Compound 2	**Compound 3**	**Ciprofloxacin**	**Compound 2**	**Compound 3**
E.coli NCTC 5933	13.0	15.0	16.0	50	25
E.coli K88	13.5	14.5	17.0	50	25
E.coli NCTC 7360	14.0	15.0	17.0	50	25
E.coli LT37	13.5	15.5	16.0	50	25
E.coli 872	14.0	15.0	16.0	50	25
E.coli ROW 7/12	14.0	15.5	16.5	50	25
E.coli 3:37C	14.5	16.0	16.5	50	25
E.coli CD/99/1	14.0	15.5	17.0	50	25
*E.coli HB101**	12.0	12.5	14.0	200	100
*E.coli C600**	11.5	13.0	13.5	200	100
Salmonella typhi Ty2	13.5	13.5	16.0	100	100
Salmonella enterica TD 01	13.5	13.5	19.0	100	100
Shigella dysentery 8	11.5	12.0	20.0	200	100
Shigella soneii 1	13.0	12.5	19.5	200	100
Shigella boydii D13629	12.0	12.0	20.0	200	100
Shigella flexneri Type 6	12.0	13.0	20.5	200	100
Staphylococcus aureus MDR10	13.5	13.0	18.0	50	50
*S.aureus MDR 1**	10.0	9.5	11.5	200	400
*S.aureus MDR 2**	11.5	10.0	12.0	200	400
Bacillus pumilus 82	6.0	6.0	19.0	NA	NA
Bacillus subtilis ATCC 6633	6.0	6.0	18.0	NA	NA
Vibrio cholerae NCTC 4693	14.0	15.5	17.5	50	25
NA; no activity					

Name of Bacteria	Zone of inhibition in mm (200 µg/ml)			MIC (µg/ml)	
	Compound 2	Compound 3	Ciprofloxacin	Compound 2	Compound 3
Vibrio cholerae NCTC5596	14.5	16.0	18.5	50	25
Vibrio cholerae NCTC 10732	14.5	16.0	19.0	50	25
Vibrio cholerae NCTC 11501	14.5	15.5	18.5	50	25
*Pseudomonas aeruginosa MDR 1**	10.5	10.0	12.5	100	400
NA; no activity					

Table 2
Zone of inhibition and minimum inhibitory concentration of the compound **2** and **3** against the tested fungal species

Name of Fungi	Zone of inhibition in mm(2000µg/ml)			MIC(µg/ml)	
	Compound 2	Compound 3	Griseofulvin	Compound 2	Compound 3
Candida albicans ATCC 10231	12.0	14.5	16.0	400	200
Aspergillus niger ATCC 6275	11.0	14.0	15.0	800	400
Penicillium notatum ATCC 11625	11.0	13.0	13.5	800	400
Penicillium funiculosum NCTC 287	10.5	13.5	14.0	800	200

In silico analysis

Molecular docking analysis

Molecular docking analysis of the synthesized compounds **2** and **3** was conducted against the *E. coli* FabI enzyme (PDB ID: 1C14) to assess their binding affinities, using triclosan as the reference ligand. Compound **2** showed a docking score of − 5.677 kcal/mol and glide energy of − 25.140 kcal/mol (Table 3). The docking results revealed that the compound occupies the catalytic pocket of FabI, as illustrated in the 2D and 3D interaction diagrams (Figs. 1 and 2). Interaction analysis revealed a hydrogen bond with Lys163 and polar interactions with Ser145 and Thr194. Additionally, several hydrophobic interactions were observed with residues Leu144, Met159, Tyr156, Phe203, Ile200, Ala197, Ala189, Met206, Ile192, Pro191, and Ile20, along with a π–cation interaction with Tyr146. These interactions

indicate favorable binding of compound **2** within the FabI active site and suggest its potential to inhibit the enzyme by occupying the NADH binding pocket.

Compound **3** showed a docking score of − 4.976 kcal/mol and a glide energy of − 29.372 kcal/mol against the FabI enzyme (Table 3). The docking pose indicated that the compound occupies the catalytic pocket of FabI, as illustrated in the 2D and 3D interaction diagrams (Figs. 3 and 4). Interaction analysis revealed a hydrogen bond with Gly93 and polar interactions with Hie90, Ser91, Ser145, and Thr194. In addition, hydrophobic interactions with lipophilic residues of the binding pocket and π–π stacking interactions with Lys163 were observed, contributing to the stabilization of the ligand within the active site. To validate the docking protocol, triclosan, a known FabI inhibitor, was redocked into the enzyme's active site under the same conditions, yielding a docking score of **− 7**.194 kcal/mol, which confirmed the reliability of the docking method.

Table 3
Docking scores and glide energy of synthesized compounds

Ligand	**Docking score (kcal/mol)**	**Glide energy (kcal/mol)**	**Key Interactions**	
			H-bonds	**None H-bonds**
Compound **2**	-5.677	-25.140	Lys163	Tyr146, Ser145, Thr194
Compound **3**	-4.976	-29.372	Gly93	Lys 163, HIE90, Ser91, Ser145, Thr194
Native ligand	-7.194	-35.771	Thr194	Lys163, Tyr146

Drug-Likeness, and ADMET properties

Drug-Likeness

Drug-likeness and physicochemical properties are important for predicting oral bioavailability and pharmacokinetic behavior of potential drug candidates. Parameters such as solubility, lipophilicity, hydrogen bonding capacity, molecular flexibility, and synthetic accessibility were evaluated based on Lipinski's Rule of Five [19,20]. The drug-likeness profiles of compounds **2** and **3** were predicted using ADMETlab 3.0 and compared with Native ligand (Table 4).

Both compounds exhibited physicochemical parameters within acceptable ranges. Compound **2** showed high aqueous solubility and moderate lipophilicity, whereas compound **3** displayed slightly higher lipophilicity but remained within acceptable limits. Both compounds satisfied Lipinski's criteria and showed favorable hydrogen bonding capacity, molecular flexibility, and topological polar surface area (TPSA = 23.47 Å²), indicating good membrane permeability [21]. High QED values and low synthetic accessibility scores further suggest strong drug-likeness and feasible synthesis. The compounds demonstrated favorable solubility and synthetic accessibility with acceptable lipophilicity.

Table 4
Physicochemical, and drug-likeness properties of the synthesized compounds

Parameters	Compound 2	Compound 3	Native ligand	Reference Range	Interpretation
nHA (H-bond acceptors)	2	1	2	0–12	Both are within acceptable range.
nHD (H-bond donors)	1	1	1	0–7	Indicates acceptable H-bonding for oral bioavailability.
nRot (rotatable bonds)	3	3	2	0–11	Suggests moderate molecular flexibility.
TPSA (Å²) (topological polar surface area)	23.47	23.47	29.46	0–140	Low TPSA, favorable for membrane permeability and oral absorption.
LogS (solubility)	-2.535	-3.469	-4.555	-4 to 0.5	Compound **2** has better aqueous solubility; both are within range.
LogP (lipophilicity)	2.789	3.774	4.512	0–3	Compound **2** has moderate lipophilicity; compound **3** is slightly above the ideal.
LogD (distribution at pH 7.4)	2.36	3.234	3.494	1–3	Both compounds show good membrane permeability; compound **3** is near upper limit.
Lipinski's Rule of 5	Accepted	Accepted	Accepted	—	Indicates good oral drug-likeness.
QED (quantity estimate of drug-likeness)	0.823	0.878	0.829	> 0.67	High QED scores indicate strong drug-like properties.
SA score (synthetic access)	2	2	1	≤ 6	Both are synthetically accessible.

ADMET Properties

In silico ADMET predictions using online ADMETlab 3.0 were conducted to evaluate the pharmacokinetic and toxicity profiles of compounds **2** and **3**, with native ligand as a reference (Table 5). Parameters assessed included absorption, distribution, metabolism, elimination, toxicity, blood-brain barrier (BBB) permeability, gastrointestinal absorption, P-glycoprotein (P-gp) interaction, and cytochrome P450 inhibition [22]. Caco-2 cell permeability is commonly used to estimate human intestinal absorption, with values above − 5.15 cm/s indicating good absorption potential. Both compounds exceeded this

threshold, suggesting strong oral absorption. The Human Intestinal Absorption (HIA) model also predicted high absorption, with both compounds scoring below 0.01. Neither compound is a P-gp substrate, suggesting minimal efflux and good oral bioavailability [23]. Volume of distribution (VDss) values were within the normal range (0.454 and 0.617 L/kg), and BBB permeability was moderate for compound **2** (0.462) but higher for compound **3** (0.66), indicating potential CNS penetration.

Metabolic predictions showed no inhibition of CYP1A2, CYP2C19, or CYP2C8 enzymes, suggesting low risk of drug–drug interactions. Both compounds displayed favorable clearance, though compound **2** had a slightly longer half-life (0.964), potentially leading to extended systemic exposure [24]. Toxicity predictions indicated low hERG inhibition and minimal p53 activation, with compound **3** exhibiting lower Ames mutagenicity than compound **2**, reflecting a slightly safer profile.

Table 5
Prediction of ADMET properties of the synthesized compounds

Parameter	Compound 2	Compound 3	Native ligand	Recommended Range	Interpretation
Caco-2 permeability	-4.765	-4.725	-4.805	> -5.15	Good intestinal permeability predicted for both.
PPB (%plasma protein bound)	82.545%	86.3%	99.158%	< 90%	Acceptable plasma protein binding.
HIA (absorption)	0.0	0.0	0.0	0.0–0.1	Good human intestinal absorption predicted.
Pgp-substrate	0.055	0.018	0.004	0.0–0.1	Low risk of P-glycoprotein efflux; favorable for oral bioavailability.
VDss (L/kg)	0.454	0.617	-0.149	0.04–20	Moderate volume of distribution.
BBB permeability	0.462	0.66	0.967	0.5–0.7	Compound **3** may cross the blood-brain barrier; compound **2** is borderline.
CYP inhibition	All values < 0.1	All values < 0.1	All values < 0.1	0.0–0.1	Both compounds are unlikely to inhibit major CYP450 enzymes favorable.
Clearance (mL/min/kg)	13.946	9.668	6.416	≥ 5	Both have acceptable drug clearance rates.
Half-life (T½)	0.964	0.465	1.139	0.3–0.7 (medium)	Compound **3** shows moderate stability; compound **2** has a slightly longer half-life.
hERG inhibition (human ether-a-go-go related gene)	0.358	0.64	0.89	0.0–0.7	Within medium risk; compound **3** closer to upper bound.
Ames test	0.413	0.248	0.246	0.0–0.3	Compound **3** shows lower mutagenic potential than **2**.
SR-p53 interaction	0.00	0.068	0.458	0.0–0.3	Low toxicity risk for both.

Parameter	Compound 2	Compound 3	Native ligand	Recommended Range	Interpretation
(a tumor suppressor protein p53)					

Conclusion

Two novel aminoalkyl derivatives of carvacrol, 4-((dimethylamino)methyl)-5-isopropyl-2-methylphenol (**2**) and 5-isopropyl-2-methyl-4-(piperidin-1-ylmethyl)phenol (**3**), were synthesized via a Mannich-type reaction. Both compounds exhibited broad-spectrum antimicrobial activity, with compound **3** showing superior potency. Notably, compound **3** inhibited *Escherichia coli* growth at MIC 25 µg/mL (versus 50 µg/mL for compound **2**), and demonstrated antifungal activity against *Candida albicans* and *Penicillium funiculosum* (MIC 200 µg/mL). Molecular docking studies indicated favorable interactions of both compounds with the *E. coli* FabI enzyme, a key target in bacterial fatty acid biosynthesis. These findings support the potential of structural modifications of carvacrol to improve its antimicrobial profile.

Declarations

Acknowledgements

A.G. thanks Addis Ababa University for supporting this research.

Author Contributions

A.G., D.B., and K.A. conceived the study. **A.G. and D.B.** performed the synthesis. **D.B.** carried out the computational analyses and interpreted the results, and also supervised the project. **A.M.** conducted the antimicrobial assays and contributed to data interpretation. **A.G.** drafted the manuscript, and **K.A. and D.B.** contributed to its revision and editing. All authors reviewed and approved the final manuscript.

Funding

No funding was received for this study.

Potential conflicts of interest

The authors declare no competing interests.

Additional information: Supplementary Information

Correspondence: Requests for materials should be addressed to A.G.

References

1. Verhoef J, van Kessel K, Snippe H. Immune Response in Human Pathology: Infections Caused by Bacteria, Viruses, Fungi, and Parasites. *Nijkamp Parnham's Princ Immunopharmacol*. Published online February 2019:165-178.
2. Metrics GH. Global burden of 369 diseases and injuries in 204 countries and territories , 1990 – 2019 : a systematic analysis for the Global Burden of Disease Study 2019. *Lancet*. 2020;396(10258):1204-1222.
3. WHO. infectious-diseases-are-spreading-more-rapidly-than-ever-before,-who-warns. Published online 2007. https://www.bcm.edu/departments/molecular-virology-and-microbiology/emerging-infections-and-biodefense/introduction-to-infectious-diseases
4. Ikuta KS et al. Global mortality associated with 33 bacterial pathogens in 2019 : a systematic analysis for the Global Burden of Disease Study 2019. *Lancet*. 2022;400(10369):2221-2248.
5. Bongomin F. Global and Multi-National Prevalence of Fungal Diseases — Estimate Precision. *J Fungi*. 2017;3(4):57.
6. Denning DW. Global incidence and mortality of severe fungal disease. *Lancet Infect Dis*. 2024;24(7):e428-e438.
7. Hao Y, Li J, Shi L. A Carvacrol-Rich Essential Oil Extracted From Oregano (Origanum vulgare "Hot & Spicy") Exerts Potent Antibacterial Effects Against Staphylococcus aureus. *Front Microbiol*. 2021;12:741861(r):1-13.
8. Baranauskaite J, Duman G, Corapcioğlu G, et al. Liposomal Incorporation to Improve Dissolution and Stability of Rosmarinic Acid and Carvacrol Extracted from Oregano (O. onites L.). *Biomed Res Int*. 2018;2018:61473:1-10.
9. Bhardwaj R, Parihar P, Yadav K, Bardhan NB, Komal Y. Synthesis, Characterization and Application of Mannich Base. *Galore Int J Appl Sci Humanit*. 2018;2(2):19.
10. Mitchell, J.K. and Carter W. Modeling Antimicrobial Activity of Clorox (R) Using an Agar-Diffusion Test: A New Twist on an Old Experiment. *Bioscene*. 2000;26(3):9-13.
11. H MSS, D HP. Antimicrobial activity and phytochemical analysis of selected Indian folk medicinal plants. *Int J Pharma Sci Res*. 2010;1(10):430-434.
12. (CLSI) C and LSI. *Methods for Dilution Antimicrobial Susceptibility Tests for Bacteria That Grow Aerobically: Approved Standard, 10th Edition. CLSI Document M07-A10. Wayne, PA: Clinical and Laboratory Standards Institute; 2015*.
13. V LB, Heithoff DM, Mahan SP, House JK, Mahan MJ. Antimicrobial susceptibility testing to evaluate minimum inhibitory concentration values of clinically relevant antibiotics. *STAR Protoc*. 2023;4(3):102512.
14. Sastry GM, Adzhigirey M, Sherman W. Protein and ligand preparation : parameters , protocols , and influence on virtual screening enrichments. *J Comput Aided Mol Des*. 2013;27(3):221-234.
15. Schrödinger L. Schrödinger Release 2023-1: LigPrep; Schrödinger, LLC: New York, NY, USA,. Published online 2023.

16. Nataro JP, Kaper JB. Diarrheagenic Escherichia coli. *Clin Microbiol Rev*. 1998;11(1):142-201.
17. Sader HS, Jones RN, Silva JB, Sentry T, Group P, America L. Skin and soft tissue infections in Latin American medical centers : four-year assessment of the pathogen frequency and antimicrobial susceptibility patterns. *Diagn Microbiol Infect Dis*. 2002;44(3):281-288.
18. Chowdhury F, Ross AG, Islam T, Mcmillan NAJ. Diagnosis , Management , and Future Control of Cholera. *Clin Microbiol Rev*. 2022;35(3):1-23.
19. Lipinski CA, Lombardo F, Dominy BW, Feeney PJ. Experimental and computational approaches to estimate solubility and permeability in drug discovery and development settings. *Adv Drug Deliv Rev*. 2001;46(1–3):3-26.
20. Serdaroğlu G. Computational Insights in Drug-likeness and ADMT Properties of -dienes Resemble of Geranial Geranial benzeri - dienlerin İlaç Benzerliği ve ADMT Özelliklerine İlişkin Hesaplamalı Analizler. *Ordu Univ J Sci Technol*. 2023;13(2):174-192.
21. Babalola S, Igie N. of p -Nitrophenyl Hydrazones as Anti-in fl ammatory Compounds against COX-2 , 5-LOX , and H þ / K þ ATPaseMolecular Docking , Drug-Likeness Analysis , In Silico Pharmacokinetics , and Toxicity Studies. *Pharm Front*. 2022;4:e250–e266.
22. Fu L, Shi S, Yi J, et al. ADMETlab 3 . 0 : an updated comprehensive online ADMET prediction platform enhanced with broader coverage , impro v ed perf ormance , API functionality and decision support. *Nucleic Acids Res*. 2024;52(W1):422-431.
23. Lin JH, Yamazaki M. Role of P-Glycoprotein in Pharmacokinetics Clinical Implications. *Clin Pharmacokinet*. 2003;42(1):59-98.
24. Benet LZ, Hoener B ann, Francisco S. Changes in plasma protein binding have little clinical relevance. *Clin Pharmacol Ther*. 2002;71(3):115-121.

Schemes

Schemes 1 and 2 are available in the Supplementary Files section

Figures

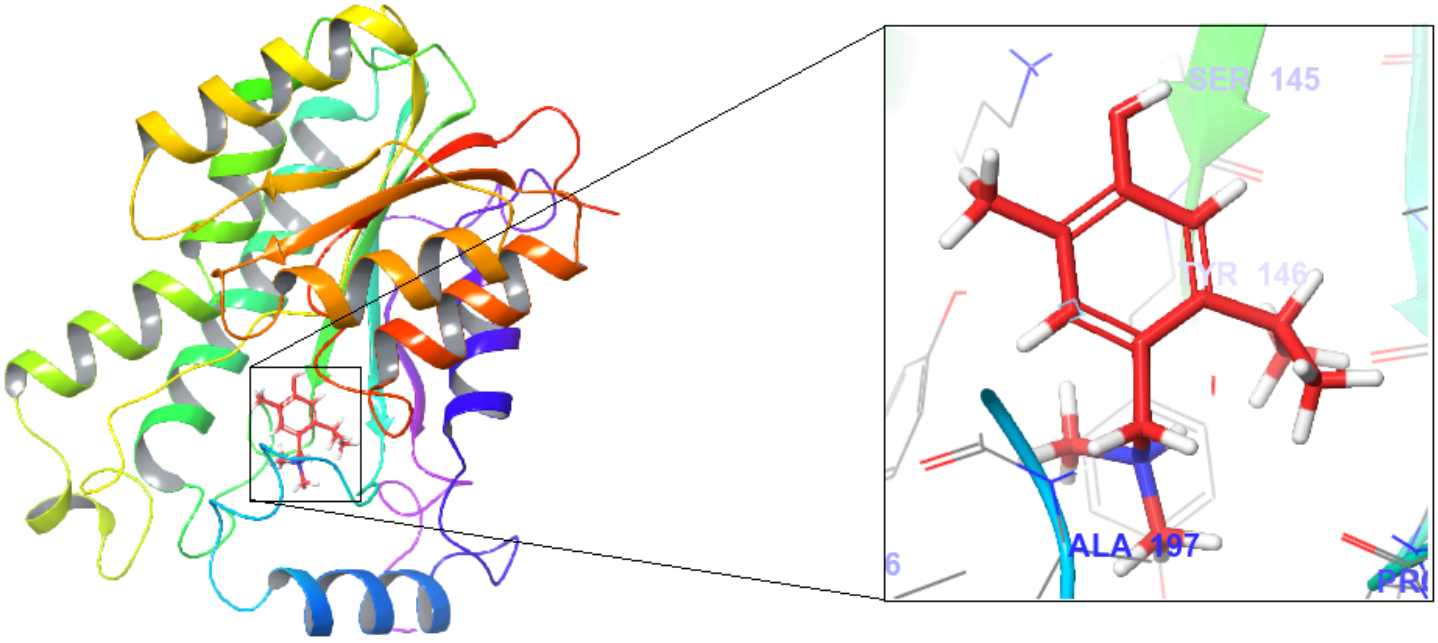


Figure 1

3D interaction between compound 2and *E. coli* FabI (PDB ID: 1C14)

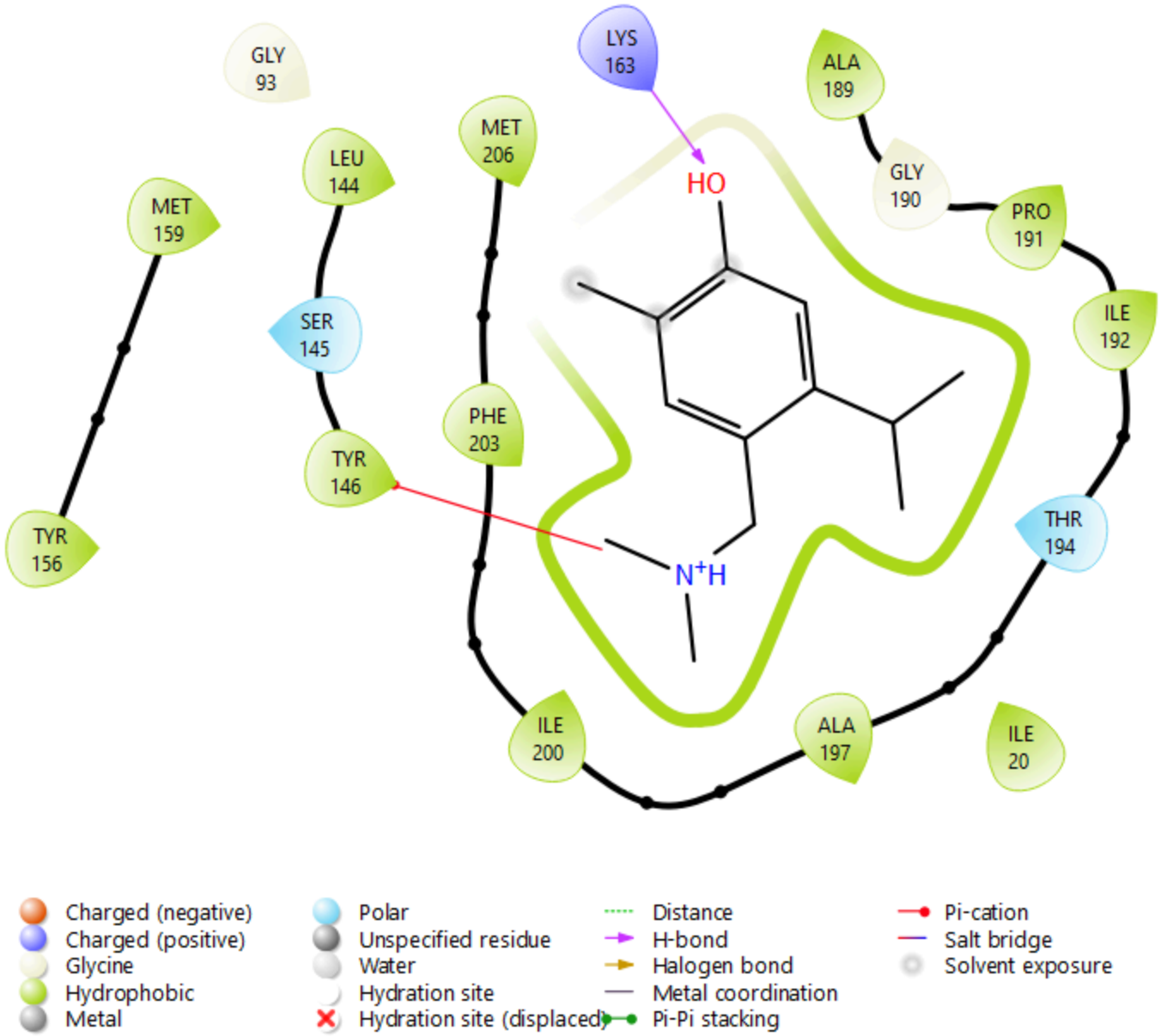


Figure 2

2D interaction between compound 2and *E. coli* FabI (PDB ID: 1C14)

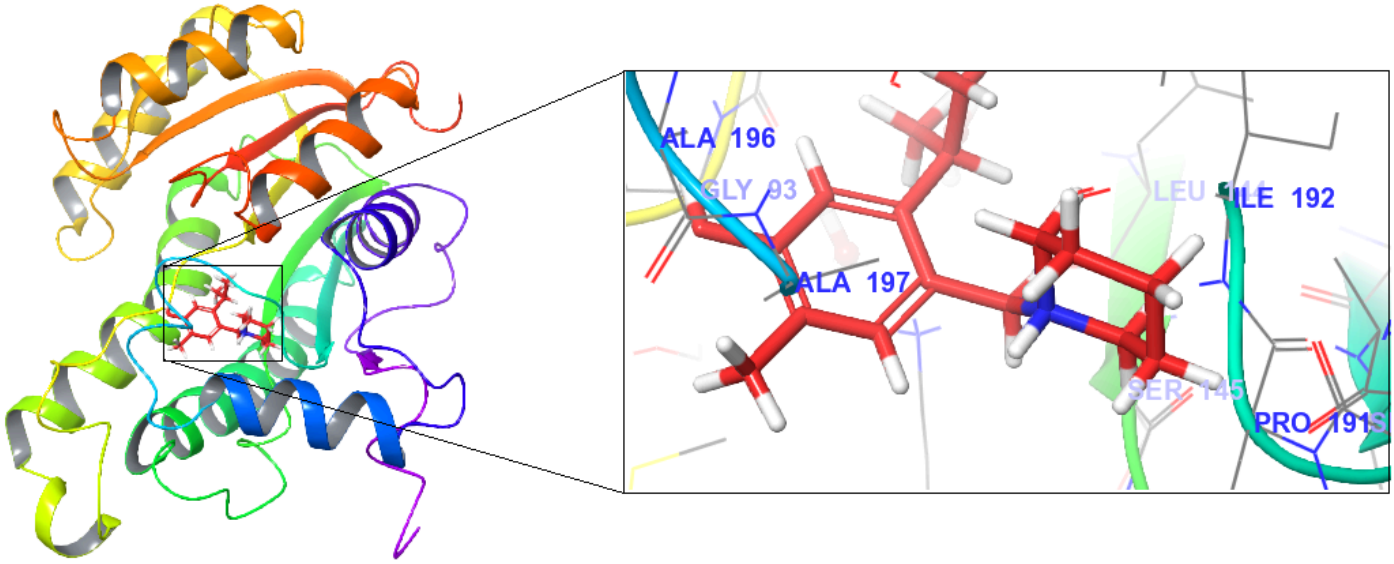


Figure 3

3D interaction between compound 3and *E. coli* FabI (PDB ID: 1C14)

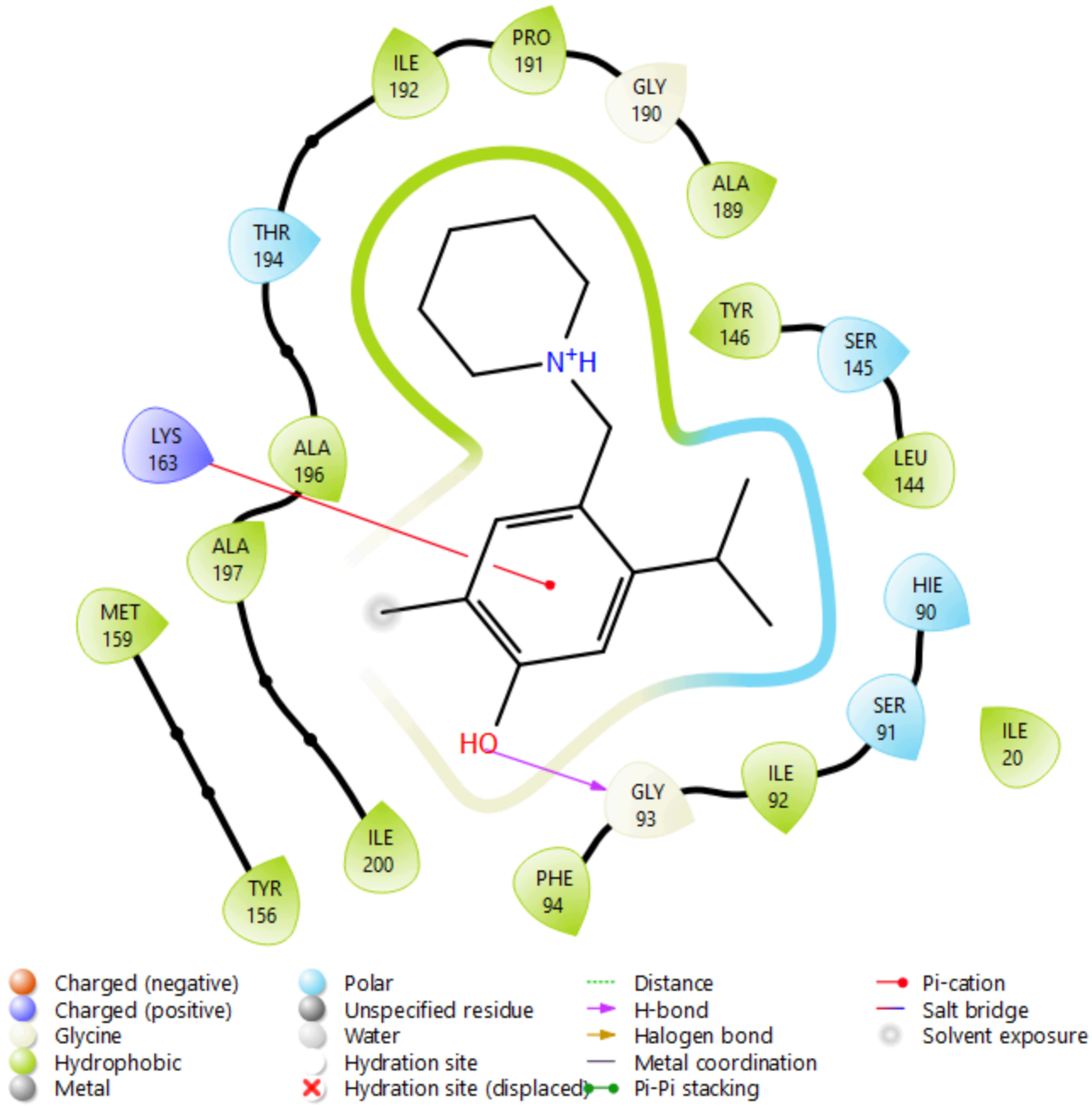


Figure 4

2D interaction between compound 3and *E. coli* FabI (PDB ID: 1C14)

Supplementary Files

This is a list of supplementary files associated with this preprint. Click to download.

- Supplementary.docx
- Schemes.docx